J. Mod. Power Syst. Clean Energy (2018) 6(1):158–167
https://doi.org/10.1007/s40565-017-0316-x

Interaction analysis between induction motor loads and STATCOM in weak grid using induction machine model

Ding WANG[1], Xiaoming YUAN[1]

Abstract Static synchronous compensators (STATCOM) can be used as a reactive power compensation for induction motor (IM) loads due to its effective control and good compensation. Terminal voltage control (TVC) in a STATCOM has a great influence on voltage dynamics which is a significant concern in a system with many IM loads. This paper investigates the interaction between IM loads and TVC in a STATCOM under weak grid conditions from the viewpoint of active and reactive power flow. A corresponding induction machine model is proposed, based on which the interaction mechanism between IM loads and TVC in a STATCOM can be intuitively understood. It is shown that the negative damping component provided by TVC in a STATCOM can lead to system oscillation instability. Grid strength and the inertia constant of the induction machine affect the extent of such interaction. Time-domain simulation results of IM loads connected to an infinite system through a long transmission line, with STATCOM compensation implemented in MATLAB/Simulink, validate the correctness of the analyses.

CrossCheck date: 2 May 2017

Received: 23 March 2016 / Accepted: 2 May 2017 / Published online: 9 September 2017

✉ Xiaoming YUAN
yuanxm@hust.edu.cn

Ding WANG
wangding@hust.edu.cn

[1] State Key Laboratory of Advanced Electromagnetic Engineering and Technology, Huazhong University of Science and Technology, Wuhan 430074, China

Keywords Induction machine, Small signal stability, Static synchronous compensator (STATCOM), Terminal voltage control, Weak grid

1 Introduction

Induction machines are an important element in power systems. About 60%–70% of industrial energy consumption is due to induction motor (IM) loads [1]. Owing to the reactive power consumption characteristics of IM loads in power systems, reactive compensation devices is necessary. For effective control and good compensation performance [2, 3], static synchronous compensators (STATCOM) are widely employed for reactive power compensation. Research on induction machines and STATCOMs is mostly concerned about low voltage ride through characteristics [4, 5], improvement of voltage sag due to starting of high power induction motor [6] and stabilizing of sub-synchronous resonance [7]. However, the interaction between IM loads and a STATCOM has not gained enough attention. Actually, terminal voltage control (TVC) in a STATCOM has a great influence on voltage dynamics which is a significant concern in a system with heavy IM loads. This phenomenon has not been studied extensively. Furthermore, long distance transmission, intensive use of transmission and the increasing number of IM loads make the system overstressed [8]. The AC grid strength which is described by the short circuit ratio (SCR) becomes weak. Since the bus voltage is more sensitive to TVC under weak grid conditions, interactions between IM loads and a STATCOM will be strengthened. Therefore, it is necessary to analyze the complex interaction between IM loads and TVC in a STATCOM under the weak grid conditions.

STATE GRID
STATE GRID ELECTRIC POWER RESEARCH INSTITUTE

Although previous work has rarely focused on this topic, there is still some similar research about the interaction between IM loads and grid-connected equipment with voltage control. Earlier studies found that the interaction between IM loads and the excitation system of synchronous generators would lead to system oscillations [9–11]. Time domain simulations, bifurcation theory and modal analysis are used in those studies to uncover the factors that affect the interaction. Nowadays, with the development of renewable energy, HVDC, FACTs, etc., more and more power electronics equipped with intricate control strategies are integrated into power system, making the power system dynamic more complicated [12]. Thus, the interactions between power electronics and IM loads tend to attract more attention [13–15]. In [13], the voltage oscillation between IM loads and DFIGs in power distribution networks is reported. The studies of [14, 15] show that the interaction of IM loads and a droop-controlled voltage source converter (VSC) in a microgrid can lead to low-frequency and medium-frequency oscillations. All this research has focused on the interaction between IM loads and grid-connected equipment with voltage control, and resulted progress in this area. However, there are few reports about the interaction analysis of IM loads and a STATCOM. Therefore, this paper concentrates on that. In order to make it easy to comprehend the internal mechanism of the interaction from physical viewpoint, the flow of active and reactive power is considered. Based on this, a corresponding induction machine model is proposed and used to reveal the internal mechanism.

The paper is structured as follows. Section 2 introduces the basic understanding for interaction. Section 3 first presents the proposed induction machine model, then the STATCOM and the network are modeled. Section 4 develops the modal analysis. Section 5 investigates the effects of TVC in the STATCOM, the grid strength and the inertia constant of the induction machine on system stability. Simulation studies are carried out in Sect. 6 to validate the above analyses. Section 7 summarizes the conclusions.

2 Basic understanding for interaction between IM loads and STATCOM

Figure 1 shows an IM load connected to an infinite grid through a long transmission line with a STATCOM compensation. The STATCOM and IM are connected to the point of common coupling (PCC). A fixed compensation capacitor for the IM is also located at the PCC bus.

In Fig. 1, U_{dcref} and U_{dc} are the voltage reference value and the measured voltage at the DC capacitor; U_{tref} and U_t are the terminal voltage reference and measured voltage;

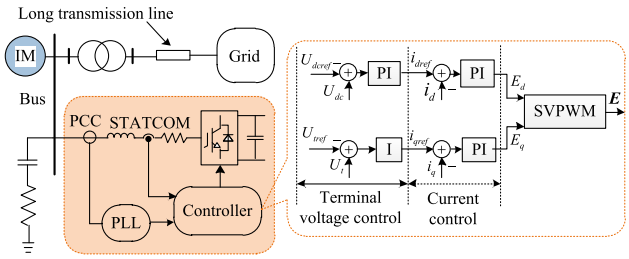

Fig. 1 Induction motor loads connected to infinite grid through long transmission line with STATCOM compensation

i_{dref} and i_{qref} are the current reference with respect to d axis and q axis; i_d and i_q are the corresponding measured values of the current in the filter inductor; E_d and E_q are the outputs of the PI regulator; E is the internal voltage vector of the VSC.

The corresponding single line diagram of the system is shown in Fig. 2. U_g is the magnitude of infinite grid voltage; L_3 is the equivalent inductance of the transformer and transmission line; $P_e + \mathrm{j}Q_e$ are active and reactive power injected into the IM; U_t and θ_{ut} are the terminal voltage magnitude and phase; C_f and R_d are fixed compensation capacitance and resistance; $P_{ec} + \mathrm{j}Q_{ec}$ are active and reactive power flowing from the fixed capacitor to the PCC bus; $P_{eg} + \mathrm{j}Q_{eg}$ are active and reactive power delivered to PCC bus by the infinite grid; $P_{e2} + \mathrm{j}Q_{e2}$ are active and reactive power sent to PCC bus by the STATCOM; L_1 and R_1 are filter inductance and resistance in the STATCOM.

We assume that the public coordinate viz. d axis is in phase with the infinite grid voltage. For clearly comprehension of the system, the power $P_{eg} + \mathrm{j}Q_{eg}$ and $P_{ec} + \mathrm{j}Q_{ec}$ (shown in Fig. 2) are combined into the power $P_{e1} + \mathrm{j}Q_{e1}$, that is $P_{e1} + \mathrm{j}Q_{e1} = (P_{eg} + \mathrm{j}Q_{eg}) + (P_{ec} + \mathrm{j}Q_{ec})$. Thus, based on the flow of active and reactive power in Fig. 2, the block diagram of the overall system is shown in Fig. 3.

It can be seen from the Fig. 3 that the input electric power of IM consists of two parts: ① the power from network, which is affected by the terminal voltage vector, the transmission line and the characteristics of capacitor; ② the power from the STATCOM, which is closely related to

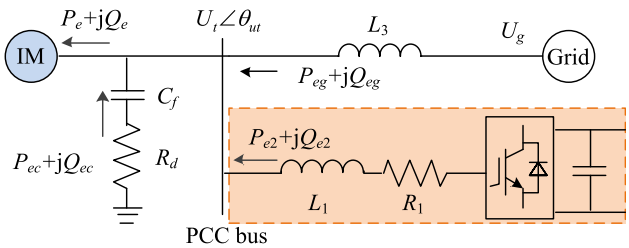

Fig. 2 Single line diagram of system

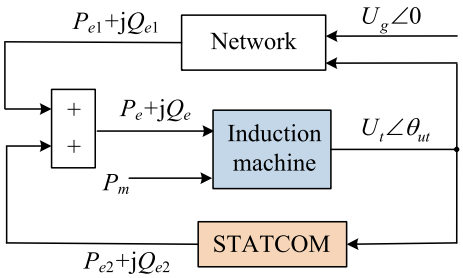

Fig. 3 Block diagram of overall system

the terminal voltage magnitude and the corresponding controller.

The interaction between the IM and the STATCOM becomes pronounced under weak grid conditions. On one hand, the power injected into the IM comes from the network and the STATCOM. If the network operates under weak grid conditions then a large amount of reactive power is provided by the STATCOM, and strong interaction between IM and STATCOM occurs. While on the other hand, also under weak grid conditions, the dynamics of terminal voltage magnitude are mainly affected by TVC in the STATCOM, which leads to the fact that the active power transferred from the network to IM relies on the dynamic performance of TVC. Thus, the interaction between the IM loads and STATCOM, which includes the reactive power exchange between IM and STATCOM and the effects of TVC on IM-received active power, make it necessary to investigate the internal mechanism.

3 System modelling for analysis

Based on the basic understanding of the interaction shown in Section 2, this section focuses on the system modelling which will be modeled from the viewpoint of active and reactive power flow. One thing that should be noted is that the problems of concern have a relatively slow timescale, which means only quasi steady state of the IM, power electronics equipment and network is considered, while transient processes are ignored [16]. The modal analysis shown in Section 4 will justify this simplification.

3.1 Proposed induction machine model

For the timescale we are concerned with, IM loads in most power system analyses are treated as variable impedances, which is a good approach for understanding IM loads separately. However, as mentioned in [17], the conventional IM model output variables, like the "slip" in a certain bus, lack physical significance in a power system. Moreover, this conventional model does not lay stress on the voltage magnitude. Actually, voltage stability in IM loads, when they cover an extensive area supplied by a large power system, is an issue of significant concern, and is related to the reactive power balancing. Thus, in order to avoid these defects and to accommodate the above mentioned interaction analysis, this paper proposes an IM model suitable for in-depth analysis.

Based on Fig. 3, the proposed IM model selects both active and reactive power flowing into the IM to be the inputs. The outputs are the terminal voltage phase and magnitude. It is noteworthy that the terminal voltage magnitude and phase are not determined only by the IM since the input active and reactive power are supplied from the external grid. However, the information of terminal voltage vector can be deduced from the characteristics of the IM. Therefore, the terminal voltage vector can be selected as the interface between the IM and the external grid. The IM model is derived as follows.

The steady-state equivalent circuit of an IM is shown in Fig. 4. $x_{s\sigma}$ and $x_{r\sigma}$ are the stator and rotor leakage reactances; x_m is the magnetizing reactance; s_{slip} is the slip; R_r is the rotor reactance.

The active and reactive power consumed by the IM depend on the slip and the terminal voltage magnitude as shown in Fig. 4. From the modelling perspective mentioned above, active power and reactive power are chosen as the model inputs, and the linearized relationship between P_e, Q_e and s_{slip}, U_t based on Fig. 4 is given by:

$$\begin{bmatrix} \Delta U_t \\ \Delta s_{slip} \end{bmatrix} = \begin{bmatrix} K_1 & K_2 \\ K_3 & K_4 \end{bmatrix} \begin{bmatrix} \Delta P_e \\ \Delta Q_e \end{bmatrix} \tag{1}$$

The formulae for the coefficients are given in Appendix A.

Rotor motion is described by the following differential equation:

$$\Delta P_e - \Delta P_m = 2H \frac{\mathrm{d}\Delta\omega_r}{\mathrm{d}t} \tag{2}$$

where ΔP_e and ΔP_m are the deviation of electrical and mechanical power; $\Delta\omega_r$ is the deviation of rotor speed; H is the inertia constant.

During the swings, the frequency of stator voltage deviates from the synchronous frequency. This is reflected in the following linearized equation:

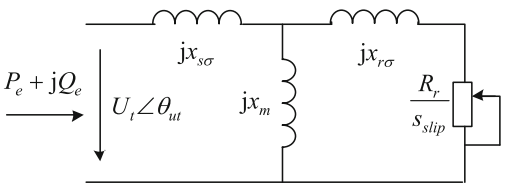

Fig. 4 Steady state equivalent circuit of induction machine

$$\Delta\omega_s = \frac{1}{1 - s_{slip0}}\Delta\omega_r + \frac{\omega_{s0}}{1 - s_{slip0}}\Delta s_{slip} \tag{3}$$

where $\Delta\omega_s$ and Δs_{slip} are the deviations of the terminal voltage frequency and slip; ω_{s0} and s_{slip0} are their respective initial states.

The integral of stator frequency is the terminal voltage phase from the physical point of view. The linearized relation is given by:

$$\omega_{s0}\Delta\omega_s = \frac{\mathrm{d}\Delta\theta_{ut}}{\mathrm{d}t} \tag{4}$$

where $\Delta\theta_{ut}$ is the deviation of the terminal voltage phase.

Based on the equations above, the linearized induction machine model is illustrated in Fig. 5. The motor convention makes ΔP_e positive and ΔP_m negative. The mechanical power is assumed to be constant in this paper.

3.2 STATCOM model

The basic function of a STATCOM is to inject reactive power to systems, which is realized using a voltage source converter. The control system of a VSC consists of: ① an inner current loop to control the filter inductor current and limit the valve current during disturbances; ② a phase locked loop (PLL) to detect the phase of the terminal voltage and establish the $dq0$ coordinate; ③ a direct-voltage control loop; ④ a terminal voltage control loop to make the PCC voltage follow the reference. The detailed control system is illustrated in Fig. 1.

On account of the timescale we are concerned with, the fast dynamic control loops in the VSC are ignored, and the following assumptions are made:

1) The inner current control loops are ignored, due to their fast response, which means the current through the filter inductor is equal to the current reference.
2) The phase locked loop is also ignored, so the PLL can instantaneously detect the phase of terminal voltage.

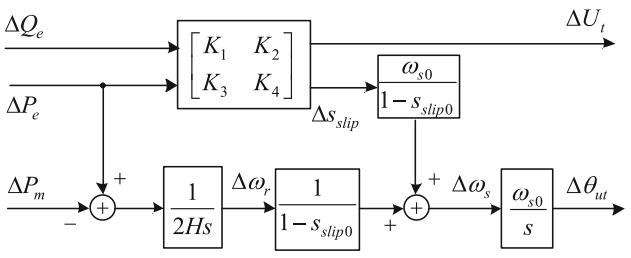

Fig. 5 Block diagram of linearized induction machine model

3) The DC voltage is constant and the STATCOM does not provide active power, so the DC voltage controller is ignored and the d axis current reference is zero.

Therefore, on the timescale of this modeling, only the TVC has a significant effect on system stability. The selection of the controller and parameters is based on the following considerations. Both an integral controller and a proportional integral controller can be employed in terminal voltage control, and the selection of the control parameters depends on the grid environment [18]. For example, in [19], a single VSC connects to an infinite grid and it is found that the terminal voltage controller's integral gain can be increased to make the system operate at its theoretical minimum SCR limit. In [20], it is derived from a VSC system that a faster outer voltage control loop will produce a less robust system. In [21], based on an entire MMC-VSC system, tuning the terminal voltage controller (TVC) parameters shows that the integral gain of the ac voltage controller needs to increase to achieve stability requirements. From the above, this paper selects an integral controller for investigation and the range of integral gain is between 20 and 120 [22]. The TVC is described as follows:

$$i_{qref} = (-U_{tref} + U_t)\frac{k_{ivt}}{s} \tag{5}$$

Under these assumptions, the active and reactive power (viz., P_{e2} and Q_{e2}) flowing from the STATCOM to the PCC bus are given by:

$$\begin{cases} P_{e2} = 0 \\ Q_{e2} = -U_t(-U_{tref} + U_t)\dfrac{k_{ivt}}{s} \end{cases} \tag{6}$$

3.3 Network model

The active and reactive power, namely P_{eg} and Q_{eg}, flowing from the infinite grid to PCC bus are:

$$\begin{cases} P_{eg} = \dfrac{U_t U_g}{x_3}\sin(-\theta_{ut}) \\ Q_{eg} = \dfrac{U_t U_g\cos(-\theta_{ut}) - U_t^2}{x_3} \end{cases} \tag{7}$$

where x_3=$\omega_s L_3$ represents the equivalent reactance of the transformer and transmission line; ω_s is the frequency of the infinite grid.

The fixed compensation capacitor provides a contribution to the total reactive power. The consumed active power is ignored as the resistance R_d in capacitor is very small. The power from capacitor is:

$$\begin{cases} P_{ec} = 0 \\ Q_{ec} = -\omega_s C_f U_t^2 \end{cases} \tag{8}$$

In summary, the power transferred to the IM is:

$$\begin{cases} P_e = \underbrace{P_{eg} + P_{ec}}_{P_{e1}} + P_{e2} \\ Q_e = \underbrace{Q_{eg} + Q_{ec}}_{Q_{e1}} + Q_{e2} \end{cases} \tag{9}$$

where P_{e1} and Q_{e1} defined above are the sum of the power from the transmission line and the capacitor.Linearizing (6)–(9) around an operating point gives:

$$\Delta P_e = K_5 \Delta U_t + K_6 \Delta \theta_{ut} \tag{10}$$

$$\Delta Q_e = K_7 \Delta U_t + K_8 \Delta \theta_{ut} \tag{11}$$

The detailed expressions of $K_5 \sim K_8$ are given in Appendix A.

4 Modal analysis

Modal analysis is a well-developed tool to determine the dominant mode that governs the system stability. Figure 6 is the eigenvalue spectrum of the power system under weak grid conditions (viz. the SCR is 1.3) with different integral gains (k_{ivt}) of TVC in the STATCOM. In order to ensure accuracy, the calculation of the pole-zero map is based on the detailed mathematic model which includes the VSC control loops and the fast dynamics of network. The parameters are shown in Table 1. In Fig. 6, the dominant pole moves from the right half plane to the left with increasing k_{ivt}. That means the system changes from unstable to stable. Therefore, TVC in the STATCOM has a crucial impact on the dominant mode. Moreover, the frequencies of the dominant eigenvalue in all the cases are

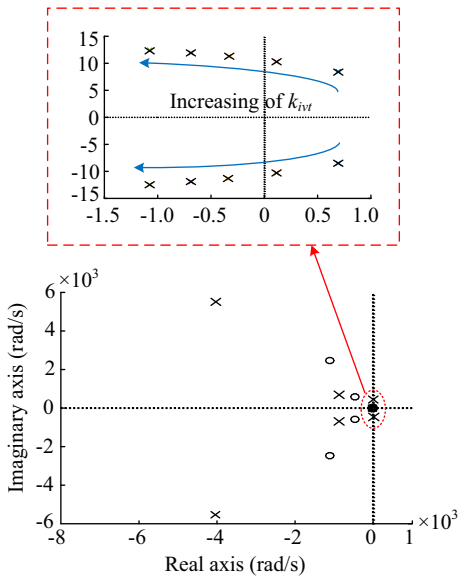

Fig. 6 Eigenvalue spectrum of system with different TVC integral gain k_{ivt}

Table 1 System parameters for modal analysis

Model	Parameters	Values
Network	Grid voltage	110 kV
	Fix capacitor	31.568 μF
	Equivalent reactance	0.2469 H
Induction machine	Rated power	3 MVA*40
	Stator resistance	0.1488 Ω
	Rotor resistance	0.0864 Ω
	Inertia constant	0.5 s
	Rated terminal voltage	12 kV
	Stator leakage inductance	1.529 mH
	Rotor leakage inductance	2.752 mH
	Magnetizing inductance	48.92 mH
STATCOM	Rated power	24 MW
	Filter inductance	0.764 mH
	Rated terminal voltage	12 kV
	Filter resistance	0.012 Ω

around 10.5 rad/s (1.6 Hz), and the damping is close to 0 when k_{ivt} is small. The participation factors of state variables shown in Table 2 suggest that the dominant mode is mainly influenced by the IM and the TVC parameters. The direct voltage control (DVC) loop and the PLL do not mainly participate in shaping of the dominant mode and hence they can be ignored in the following analysis.

The eigenvalue spectrum and participation factors indicate that there is highly dynamic interaction between the IM and TVC in the STATCOM, and also that TVC mainly affects the damping. Therefore, similarly to the model used by Heffron and Phillips [23], the system model can be simplified as follows.

Considering (10), (11) and the linearized IM model shown in Fig. 5, the system small-signal analysis model is shown in Fig. 7. By regarding $\Delta\theta_{ut}$ as the input, ΔP_e and Δs_{slip} as the outputs, the shaded area shown in Fig. 7 can be simplified into transfer functions $G_1(s)$ and $G_2(s)$.

Because the initial state of slip s_{slip0} is close to zero and the initial state of terminal voltage frequency ω_{s0} is close to 1 p.u., the small-signal analysis model shown in Fig. 7 can be transformed into Fig. 8. $G_1(s) = \Delta\theta_{ut}/\Delta P_e$, $G_2(s) = \Delta\theta_{ut}/\Delta s_{slip}$. Detailed expressions for these transfer functions are given in the Appendix A.

Table 2 Participation of state variables in mode ($k_{ivt} = 120$)

Mode	TVC	DVC	PLL		IM	
	Δi_{qref}	ΔU_{dc}	$\Delta\theta_{PLL}$	Δx_{pll}	$\Delta\omega_r$	$\Delta\theta_{ut}$
$-0.6 - j11.98$	0.144	0.031	0.021	0.021	0.392	0.309

Note: Δi_{qref} and ΔU_{dc} are the status of TVC and DVC; $\Delta\theta_{pll}$ and Δx_{pll} are the PLL's status

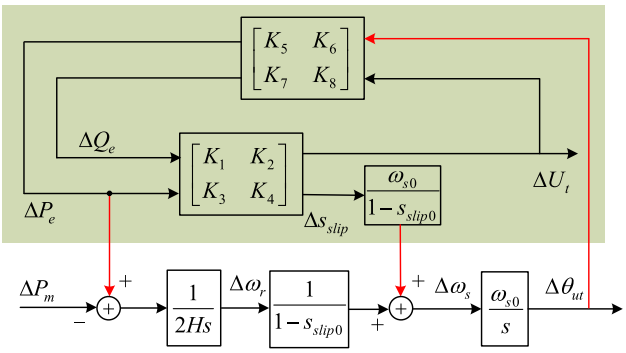

Fig. 7 Small-signal analysis model

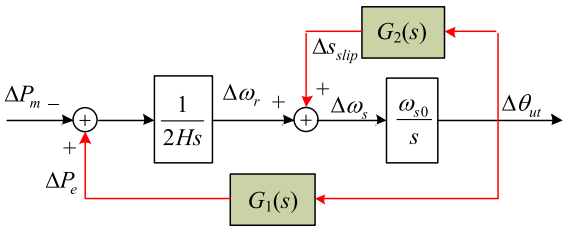

Fig. 8 Simplified analysis model for analyzing effect of TVC in STATCOM on IM

From Fig. 8, the rotor speed ω_r accelerates or decelerates when there is an unbalance between IM input and output power. Then small variations of stator speed $\Delta\omega_s$ change the terminal voltage phase θ_{ut} which influences the feedback electric power P_e and slip s_{slip} through $G_1(s)$ and $G_2(s)$ respectively. Hence, the system stability is determined by $G_1(s)$ and $G_2(s)$.

5 Stability analyses

This section elaborates several aspects of the small-signal stability of the system based on the simplified analysis model developed above. TVC in the STATCOM can influence the stability of the IM through its contribution to the damping component of the system. Meanwhile, the grid strength increases or decreases this interaction, as will be further discussed below. The effect of the inertia constant representing the mass of induction machine is also investigated.

5.1 Effect of TVC on system stability

The characteristics of $G_1(s)$ and $G_2(s)$ are closely related to the integral gain of TVC in the VSC. With constant grid conditions, $G_1(s)$ and $G_2(s)$ are investigated with different integral gains. Since small-signal stability is due to

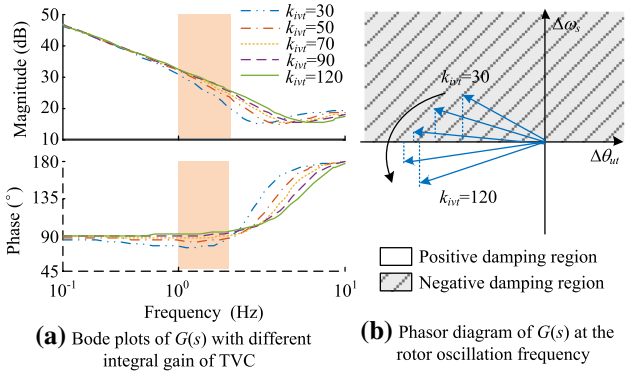

(a) Bode plots of $G(s)$ with different integral gain of TVC

(b) Phasor diagram of $G(s)$ at the rotor oscillation frequency

Fig. 9 The effect of TVC on system stability, (**a**) Bode plots of $G(s)$ with different integral gain of TVC, (**b**) phasor diagram of $G(s)$ at the rotor oscillation frequency

insufficient damping of oscillations to a great extent, we focus on the damping torque provided by $G_1(s)$ and $G_2(s)$ together. $G(s)$ denotes the transfer function from the stator speed to electromagnetic power:

$$G(s) = 2H\omega_{s0}G_2(s) + \frac{\omega_{s0}}{s}G_1(s) \tag{12}$$

The effect of TVC on system stability is investigated through the magnitude and phase frequency characteristics of the transfer function $G(s)$.

Bode plots of $G(s)$ with different integral gains of TVC are given in Fig. 9a. Corresponding phasor diagrams of $G(s)$ is illustrated in Fig. 9b. Due to the motor convention, the damping component is negative when $G(s)$ is in phase with $\Delta\omega_s$ and vice versa. The negative damping region indicates that the electromagnetic power increases when the stator speed increases, and the change of electromagnetic power is adverse to stator speed stability. On the other hand, the positive damping region indicates that the electromagnetic power decreases as the stator speed increases, and the change of electromagnetic power is beneficial for stator speed stability. As shown in Fig. 9a, when the integral gain of TVC shifts from 30 to 120, the phase frequency response corresponding to the rotor oscillation frequency, namely the shadowed part of the Bode plots, increases and finally becomes larger than 90°. Correspondingly, the damping component at the rotor oscillation frequency changes from negative to positive. Moreover, the magnitude frequency response also increases as the integral gain increases.

In summary, the damping component increases with the increase of the integral gain. Note that the integral gain cannot increase without limit due to constraints of coordinated control. The PLL and the DVC loop restrain the upper limit of integral gain of TVC. It is quite a complex question that is beyond the scope of this paper.

5.2 Effect of grid strength on system stability

The effect of the grid strength on system stability is to increase or decrease the interaction between IM loads and TVC in the STATCOM. A stronger grid has a greater influence on the dynamics of terminal voltage magnitude. This makes the system more stable and defends against small-signal disturbances.

Figure 10 illustrates the variation of the real part of the minimum system eigenvalue, as well as the corresponding damping ratio, with respect to different integral gains and SCRs, with the SCR representing the grid strength. The shaded area in the figure corresponds to negative real part of the minimum eigenvalue and therefore positive damping ratio which indicates stable operation region. The damping ratio scale in this figure is an approximate calculation. It can be seen from Fig. 10 that the curve moves down with increasing grid strength, which means the system can tolerate a larger range of integral gain.

5.3 Effects of inertial constant on system stability

The inertia of induction machines is generally close to 0.5 s [8, 24]. In order to investigate the effects of the inertia constant on system stability, an open loop transfer function has been derived based on Fig. 8. $G_{open}(s)$ denotes the open loop transfer function and is given below

$$G_{open}(s) = \frac{-G_1(s)}{2Hs\left(\frac{s}{\omega_{s0}} - G_2(s)\right)} \tag{13}$$

The inertia constant H only appears in the denominator of (13). Thus, the phase of the open loop transfer function is constant with respect to the inertia constant, while increasing the inertia constant will decrease the amplitude frequency gain and this stabilizes the system. In addition to changing the system stability, the inertia constant also affects the oscillation frequency which can be observed in the simulation results.

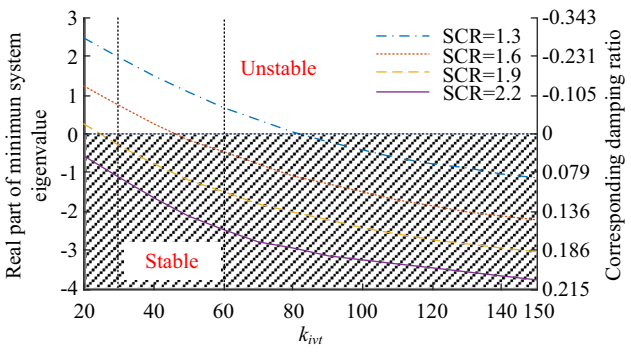

Fig. 10 Real part of minimum system eigenvalue and corresponding damping ratio with respect to different integral gains and SCRs

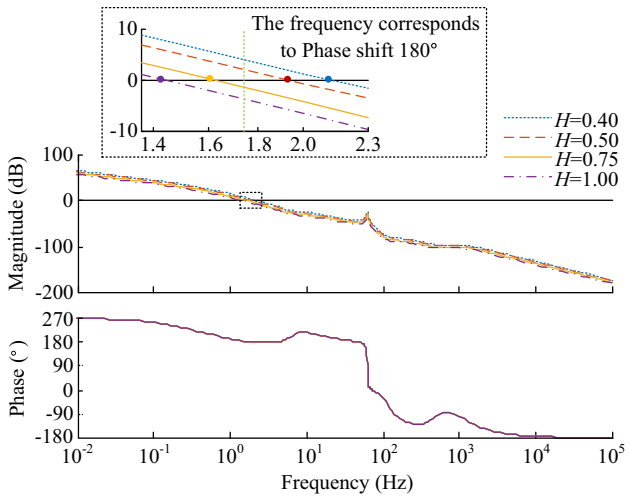

Fig. 11 Bode plots of open loop transfer function with varied inertia constant

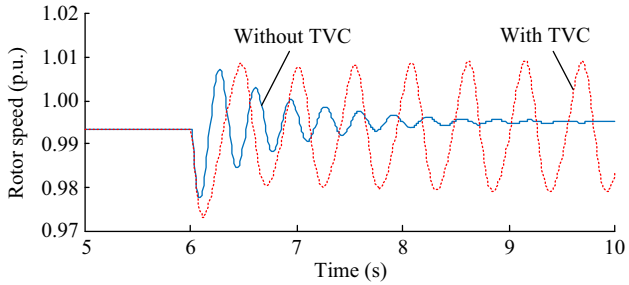

Fig. 12 Comparison of rotor speed responses for STATCOM equipped with TVC and constant q axis current control (SCR = 1.3)

Figure 11 shows the effect of the induction machine inertia on the Bode plot of $G_{open}(s)$ where k_{ivt} is 50. These Bode plots are sufficient to evaluate the system stability because there is no right-half-plane pole of $G_{open}(s)$. It is clear from the Bode plots that the phase frequency responses are identical with varying inertia constant. As the inertia constant decreases, the point where the amplitude of $G_{open}(s)$ intersects with 0 dB shifts from left to the right, and the phase corresponding to this point gradually passes through the value of 180°. That means the system becomes more unstable as the inertia constant decreases.

6 Simulation results

Based on the topology shown in Fig. 1, time-domain simulation was conducted in MATLAB/Simulink to validate the analyses described in the previous section. Parameters have been listed in Table 1.

Figure 12 compares induction machine rotor speed responses for a STATCOM equipped with TVC and

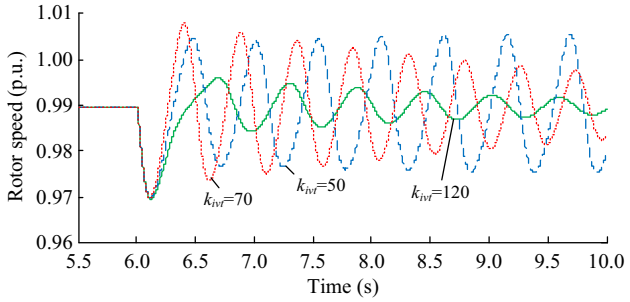

Fig. 13 Rotor speed responses of induction machine with different integral gains used for terminal voltage control

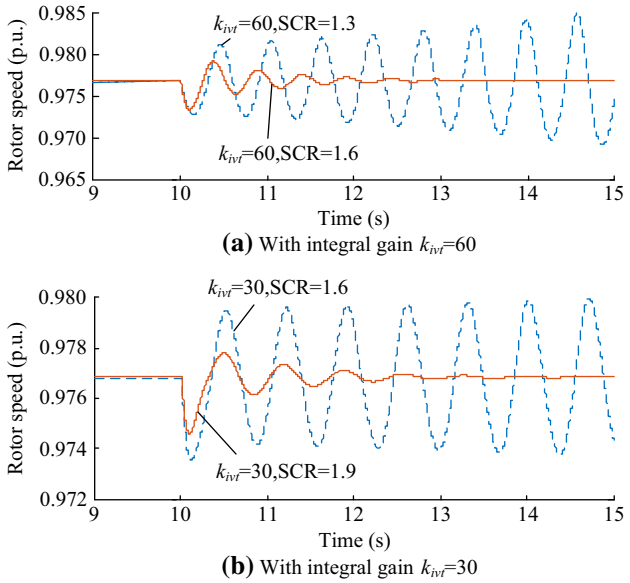

Fig. 14 Rotor speed responses compared with different grid strengths

constant q axis current control. The IM rotor speed is unstable with TVC and stable without it. Interaction between IM loads and TVC in the STATCOM may lead system to instability in a weak grid.

Figure13 is the rotor speed responses of induction machine with different integral gain of terminal voltage control. A small disturbance in grid occurs at 6 s. It can be seen from the figure that with the increase of integral gain, the stability of the system gets better. Simulation results in Fig. 13 are in accordance with the conclusion from Fig. 9. As a whole, these results illustrate that in weak grid, the damping of system oscillations is affected by terminal voltage control. Selecting suitable TVC parameters in such cases needs careful consideration.

Figure 14 shows the influence of integral gain on rotor speed stability for different grid strengths. With integral gain of 60 in Fig. 4a the system is stable with SCR = 1.6, while with integral gain of 30 in Fig. 4b the system is unstable with the same SCR. With increasing grid strength,

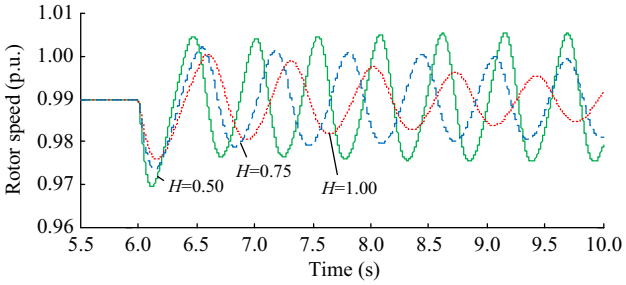

Fig. 15 Rotor speed responses with varying inertia constant

the system stability gets better, but rotor speed oscillations still last for several seconds. Overall, the simulation results are in accordance with the theoretical analysis.

Figure 15 shows the rotor speed responses with different inertia constants. When the inertia constant is 0.5 the system is unstable after a disturbance in grid, while for higher inertial constants it is stable. These simulation results support the conclusion obtained from Fig. 10.

7 Conclusion

This paper analyzed the interaction between induction motor loads and a STATCOM in a weak grid. An induction machine model was proposed to investigate the internal mechanism that causes this interaction. The results show that the stability of such systems, containing IM loads and a STATCOM, under weak grid conditions is determined by the terminal voltage controller parameters. As a consequence, it is necessary to reconsider the parameters of the VSC terminal voltage controller in systems containing substantial IM loads. Overall conclusions are as follows.

1) Terminal voltage control has a negative damping effect on stability of such systems. Decreasing the integral gain of the TVC deteriorates the system stability.
2) The grid strength determines the extent of interaction. With decreasing grid strength, as measured by the short circuit ratio, the negative damping component provided by the TVC increases. Therefore, the integral gain parameter of the TVC in a weak grid should be larger than that in a stiff grid for stable operation.
3) The inertia constant of the induction machine determines the frequency range of the interaction. Increasing the inertia constant decreases the oscillation frequency and improves the system stability.

Acknowledgements This work was supported in part by National Basic Research Program of China (973 Program) (No. 2012CB215100), Major Program of National Natural Science Foundation of China (No. 51190104) and National Natural Science Fund for Excellent Young Scholars (No. 51322704).

Appendix A

Detailed formulae for linearized IM model coefficients and transfer function are as follows:

$$K_1 = \frac{U_{t0}(P_{e0}^2 - Q_{e0}^2)}{2P_{e0}(P_{e0}^2 + Q_{e0}^2)} - \frac{U_{t0}}{2s_{slip0}} \frac{(R_r^2 - s_{slip0}^2 L_{rr}^2)\left(R_r^2 + s_{slip0}^2 L' L_{rr}\right) L_{ss}}{(R_r^2 + s_{slip0}^2 L_{rr}^2)(2P_{e0} s_{slip0} L' L_{rr} L_{ss} - Q_{e0} R_r L_m^2)} \tag{A1}$$

$$K_2 = \frac{U_{t0} Q_{e0}}{(P_{e0}^2 + Q_{e0}^2)} + \frac{U_{t0}}{2} \frac{(R_r^2 - s_{slip0}^2 L_{rr}^2) L_m^2 R_r}{(R_r^2 + s_{slip0}^2 L_{rr}^2)(2P_{e0} s_{slip0} L' L_{rr} L_{ss} - Q_{e0} R_r L_m^2)} \tag{A2}$$

$$K_3 = -\frac{R_r^2 L_{ss} + s_{slip0}^2 L' L_{rr} L_{ss}}{2P_{e0} s_{slip0} L' L_{rr} L_{ss} - Q_{e0} R_r L_m^2} \tag{A3}$$

$$K_4 = \frac{R_r s_{slip0} L_m^2}{2P_{e0} s_{slip0} L' L_{rr} L_{ss} - Q_{e0} R_r L_m^2} \tag{A4}$$

$$K_5 = -\frac{U_{g0} \sin(\theta_{ut0})}{x_3} \tag{A5}$$

$$K_6 = -\frac{U_{t0} U_{g0} \cos(\theta_{ut0})}{x_3} \tag{A6}$$

$$K_7 = \frac{U_{g0} \cos(\theta_{ut0}) - 2U_{t0}}{x_3} + \frac{k_{ivt}}{s}(U_{tref} - 2U_{t0}) - 2\omega C_f U_{t0} \tag{A7}$$

$$K_8 = -\frac{U_{t0} U_{g0} \sin(\theta_{t0})}{x_3} \tag{A8}$$

$$G_1(s) = \frac{K_6 + K_2(K_5 K_8 - K_7 K_6)}{1 - (K_1 K_5 + K_2 K_7)} \tag{A9}$$

$$G_2(s) = \frac{(K_5 K_8 - K_7 K_6)(K_2 K_3 - K_4 K_1)}{1 - (K_1 K_5 + K_2 K_7)} + \frac{(K_3 K_6 + K_4 K_8)}{1 - (K_1 K_5 + K_2 K_7)} \tag{A10}$$

References

[1] Kundur P (1994) Power system stability and control. McGraw Hill, New York

[2] Qi L, Langston J, Steurer M (2008) Applying a STATCOM for stability improvement to an existing wind farm with fixed-speed induction generators. In: Proceedings of the 2008 IEEE power and energy society general meeting, Pittsburgh, PA, USA, 1–6 July 2008, 6 pp

[3] Salles MBC, Freitas W, Morelato A (2004) Comparative analysis between SVC and DSTATCOM devices for improvement of induction generator stability. In: Proceedings of the 12th IEEE mediterranean electrotechnical conference, Dubrovnik, Croatia, 12–15 May 2004, pp 1025–1028

[4] Molinas M, Suul JA, Undeland T (2007) A simple method for analytical evaluation of LVRT in wind energy for induction generators with STATCOM or SVC. In: Proceedings of the 2007 power electronics and applications conference, Aalborg, Denmark, 2–5 Sept 2007, 10 pp

[5] Suul JA, Molinas M, Undeland T (2010) STATCOM-based indirect torque control of induction machines during voltage recovery after grid faults. IEEE Trans Power Electron 25(5):1240–1250

[6] Huweg AF, Bashi SM, Mariun N (2004) A STATCOM simulation model to improve voltage sag due to starting of high power induction motor. In: Proceedings of the 2004 power and energy conference, Kuala Lumpur, Malaysia, 29–30 Nov 2004, pp 148–152

[7] Abdou AF, Abu-Siada A, Pota HR (2011) Damping of subsynchronous oscillations and improve transient stability for wind farms. In: Proceedings of the 2011 IEEE power and energy society general meeting, Perth, WA, USA, 13–16 Nov 2011, 6 pp

[8] Leon JAD, Taylor CW (2002) Understanding and solving short-term voltage stability problems. In: Proceedings of the 2002 IEEE power engineering society summer meeting, Chicago, IL, USA, 21–25 July 2002, pp 745–752

[9] Mello FPD, Feltes JW (1996) Voltage oscillatory instability caused by induction motor loads. IEEE Trans Power Syst 11(3):1279–1285

[10] Nomikos BM, Potamianakis EG, Vournas CD (2005) Oscillatory stability and limit cycle in an autonomous system with wind generation. In: Proceedings of the IEEE power tech conference, St. Petersburg, Russia, 27–30 June 2005, 6 pp

[11] Roy NK, Pota HR, Mahmud MA (2013) Key factors affecting voltage oscillations of distribution networks with distributed generation and induction motor loads. Int J Electr Power Energy Syst 53(1):515–528

[12] Yuan XM, Cheng SJ, Hu JB (2016) Multi-time scale voltage and power angle dynamics in power electronics dominated large power systems. Proc CSEE 36(19):5145–5154

[13] Roy NK, Pota HR, Sayeef S (2013) Voltage oscillations in power distribution networks in the presence of DFIGs and induction motor loads. In: Proceedings of the IEEE power tech conference, Grenoble, France, 16–20 June 2013, pp 1–5

[14] Kahrobaeian A, Mohamed ARI (2013) Analysis and mitigation of low-frequency instabilities in autonomous medium-voltage converter-based microgrids with dynamic loads. IEEE Trans Ind Electron 1(8):1643–1658

[15] Radwan AAA, Mohamed ARI (2014) Stabilization of medium-frequency modes in isolated microgrids supplying direct online induction motor loads. IEEE Trans Smart Grid 5(1):358–370

[16] Zhao M, Yuan X, Hu J et al (2016) Voltage dynamics of current control time-scale in a VSC-connected weak grid. IEEE Trans Power Syst 31(4):2925–2937

[17] Lesieutre BC, Sauer PW, Pai MA (1995) Development and comparative study of induction machine based dynamic P, Q load models. IEEE Trans Power Syst 10(1):182–191

[18] Harnefors L, Bongiorno M, Lundberg S (2007) Input-admittance calculation and shaping for controlled voltage-source converters. IEEE Trans Ind Electron 54(6):3323–3334
[19] Ding H, Fan S, Zhou JZ et al (2015) Parametric analysis of the stability of VSC-HVDC converters. In: Proceedings of 11th IET international conference on AC and DC power transmission, Birmingham, UK, 10–12 Feb 2015, 6 pp
[20] Ho TCY, Li R, Garcia-Cerrada A et al (2013) Voltage source converter AC voltage controller design and dynamic response for a large offshore wind farm network. In: Proceedings of 2013 international conference on renewable energy research and applications, Madrid, Spain, 20–23 Oct 2013, pp 470–475
[21] Arunprasanth S, Annakkage UD, Karawita C et al (2016) Generalized frequency domain controller tuning procedure for VSC systems. IEEE Trans Power Deliv 31(2):732–742
[22] Clark K, Miller NW, Sanchez-Gasca JJ (2010) Modeling of GE wind turbine-generators for grid studies, Version 4.5. GE International Inc, Schenectady, NY, USA
[23] Heffron WG, Phillips RA (1952) Effect of a modern amplidyne voltage regulator on underexcited operation of large turbine generators. AIEE Trans Power Appar Syst 71(1):692–697
[24] Nomikos BM, Vournas CD (2005) Investigation of induction machine contribution to power system oscillations. IEEE Trans Power Syst 20(2):916–925

Ding WANG is currently working toward the Ph.D. degree with the State Key Laboratory of Advanced Electromagnetic Engineering and Technology, School of Electrical and Electronic Engineering, Huazhong University of Science and Technology, Wuhan, China. Her current research interests include stability analysis of grid-connected voltage-sourced converter and power system voltage stability analysis.

Xiaoming YUAN received the B.Eng. degree from Shandong University, China, the M.Eng. degree from Zhejiang University, China, and the Ph.D. degree from Federal University of Santa Catarina, Brazil, in 1986, 1993, and 1998 respectively, all in electrical engineering. He was with Qilu Petrochemical Corporation, China, from 1986 to 1990, where he was involved in the commissioning and testing of relaying and automation devices in power systems, adjustable speed drives, and high-power UPS systems. From 1998 to 2001, he was a Project Engineer at the Swiss Federal Institute of Technology Zurich, Switzerland, where he worked on flexible-ac-transmission-systems (FACTS) and power quality. From 2001 to 2008, he was with GE GRC Shanghai as a Manager of the Low Power Electronics Laboratory. From 2008 to 2010, he was with GE GRC US as an Electrical Chief Engineer. His research field involves stability and control of power system with multi machines multi converters, control and grid-integration of renewable energy generations, and control of high voltage dc transmission systems. He is Distinguished Expert of National Thousand Talents Program of China, and Chief Scientist of National Basic Research Program of China (973 Program). He received the first prize paper award from the Industrial Power Converter Committee of the IEEE Industry Applications Society in 1999.